A&A 537, A74 (2012)
DOI: 10.1051/0004-6361/201118205

Astronomy & Astrophysics

Oscillator strengths for lines of astrophysical interest in Rh II*

P. Quinet[1,2], E. Biémont[1,2], P. Palmeri[1], L. Engström[3], H. Hartman[4], H. Lundberg[3], and H. Nilsson[4]

[1] Astrophysique et Spectroscopie, Université de Mons – UMONS, 7000 Mons, Belgium
e-mail: quinet@umons.ac.be
[2] IPNAS, Université de Liège, Sart Tilman, 4000 Liège, Belgium
[3] Department of Physics, Lund University, PO Box 118, 221 00 Lund, Sweden
[4] Lund Observatory, Lund University, PO Box 43, 221 00 Lund, Sweden

Received 4 October 2011 / Accepted 24 October 2011

ABSTRACT

Aims. This work reports oscillator strengths for transitions of astrophysical interest in singly ionized rhodium.
Methods. Seventeen radiative lifetimes in Rh^+ have been measured with the time-resolved laser-induced fluorescence technique and combined with theoretical branching fractions calculated using a relativistic Hartree-Fock model including core-polarization effects to obtain oscillator strengths.
Results. On the basis of the good agreement between theory and experiment for the lifetimes, new reliable oscillator strengths have been deduced for a set of 113 Rh II transitions in the spectral range 153–418 nm.

Key words. atomic processes – atomic data

1. Introduction

The investigation of high resolution astronomical spectra depends directly on reliable atomic data such as transition probabilities and oscillator strengths. Although many data are now available from modern experimental techniques or sophisticated theoretical methods, they are still insufficient to meet all the needs of astrophysicists. This is particularly true for singly ionized rhodium for which no radiative data have been published so far in the literature despite the fact that several Rh II lines have been identified in different astrophysical spectra such as the solar spectrum (Moore et al. 1966) and the spectra of the HgMn type star χLupi (Lundberg et al. 1998), the super-rich mercury star HD 65949, the HgMn star HD 175640 and the peculiar Przybylski's star HD 101065 (Cowley 2009). As examples, for the three latter stars, lines observed at λ = 309.35, 316.22, 318.79, 320.73, 324.05, 330.74 and 347.78 nm were identified as radiative transitions in Rh II.

Rhodium has one stable isotope, ^{103}Rh, and 19 short-lived isotopes and isomers. In stellar nucleosynthesis, it is produced by both the *r*- and *s*-processes. The spectrum of singly ionized rhodium belongs to the Ru I isoelectronic sequence with $4d^8\ ^3F_4$ as the ground state. The laboratory term analysis was performed by Sancho (1958) who classified 814 spectral lines extending from 118.7 to 328.8 nm and established a list of 36 even and 84 odd energy levels belonging to the $4d^8$, $4d^7 5s$ and $4d^7 5p$ configurations. This work was taken as reference in subsequent atomic data compilations by Moore (1971), Meggers et al. (1975) and Reader et al. (1980). To our knowledge, the only determination of experimental transition probabilities in Rh II is due to Corliss & Bozman (1962) but their arc measurements have been recognized to be affected by large systematic errors.

In the present paper, we report on time-resolved laser-induced fluorescence (TR-LIF) lifetime measurements for 17 levels in Rh II. These new experimental lifetimes have been used to assess the reliability of theoretical results obtained within the framework of the relativistic Hartree-Fock (HFR) approach (Cowan 1981) modified by the inclusion of core-polarization effects (HFR+CPOL) (Quinet et al. 1999). From the combination of experimental lifetimes and theoretical branching fractions, it has been possible to obtain a new set of semi-empirical oscillator strengths for selected transitions of astrophysical interest. This work is an extension to longer wavelengths of our recent paper focused on VUV lines in singly ionized rhodium (Quinet et al. 2011).

2. Radiative lifetime measurements

The experimental setup used in the present experiments has been described elsewhere (Bergström et al. 1988; Xu et al. 2004; Nilsson et al. 2010) and only a brief description will be given here. The lifetime measurements were performed on ions in a laser-generated plasma employing the time-resolved laser-induced-fluorescence technique. Nd-YAG laser pulses at 532 nm with a duration of 10 ns were focused onto the surface of a rotating rhodium target in a vacuum chamber with a background pressure of about 10^{-5} mbar. For the excitation of the investigated levels, the expanding rhodium plasma was crossed at right angle by a pulsed laser beam tuned to a resonant transition of the upper level of interest. The laser used a DCM dye and was pumped by a second Nd:YAG laser. The pump laser pulses had a duration of 10 ns and were compressed to about 1.5 ns utilizing stimulated Brillouin scattering in a water cell. The two Nd:YAG lasers were synchronized by a pulse generator and had a repetition rate of 10 Hz. For the selective excitation of the investigated Rh^+ levels the corresponding wavelengths were achieved using the third harmonic of the red dye laser light, obtained by harmonic

* Table 3 is also available at the CDS via anonymous ftp to cdsarc.u-strasbg.fr (130.79.128.5) or via http://cdsarc.u-strasbg.fr/viz-bin/qcat?J/A+A/537/A74

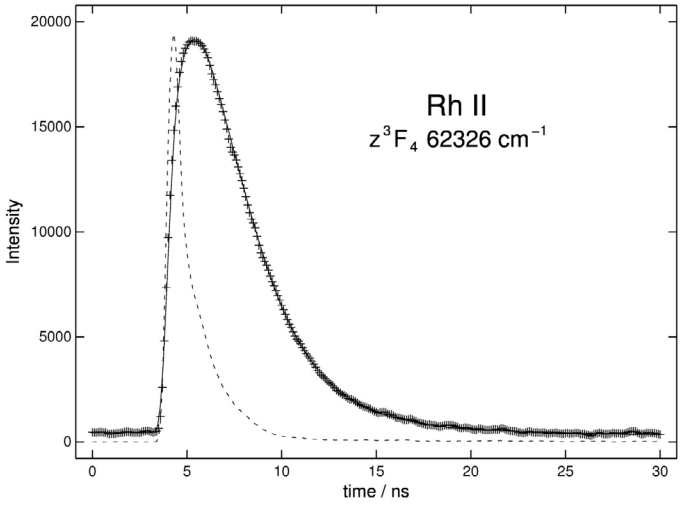

Fig. 1. Decay of the $4d^7(^4F)5p\ z^3F^\circ_4$ level at 62 326 cm^{-1}, with an evaluated lifetime of 2.4 ± 0.2 ns. Background subtracted data points with typical error bars are plotted together with a fitted single exponential decay convoluted by the measured laser pulse (solid line). The actual measurement covers more than 90 ns. The dashed curve shows the recorded laser pulse with a *FWHM* of 1.1 ns.

generation in KDP and BBO crystals and, if necessary, shifted by stimulated Raman scattering in hydrogen gas. In the measurements metastable levels of the same parity as the ground level were used as starting point for the selective excitation. These levels, with energies between 16 885 and 20 647 cm^{-1}, are only populated in an early stage of the plasma expansion. The measurements were performed about 5 mm above the target and the delay between the plasma-generating and excitation pulses was around 300 ns. This corresponds to an ion velocity larger than 10^4 m/s in the expanding plasma.

The TR-LIF signal was selected by a 1/8 m monochromator, detected by a fast photomultiplier tube with rise time 0.15 ns and digitized by an oscilloscope with 2.5 GHz analogue bandwidth. The temporal shape of the exciting laser pulses was recorded simultaneously using a photo diode. Each pair of curves were formed by averaging over 1000 laser pulses and then transferred to a PC for further treatment. The lifetimes were obtained after fitting the LIF curve with an exponential convoluted with the recorded laser pulse. An example of an experimental recording is shown in Fig. 1. In Table 1 the lifetime values are given together with the lower level used for the selective excitation, excitation wavelength, non-linear processes to obtain this wavelength from a red dye laser and strongest detection channel. Whenever possible recordings were made on several detection wavelengths. The lifetime values are averages of more than 10 recordings performed at at least two different occasions. The uncertainties in the table are mainly due to variation in results between repeated measurements and possible systematic errors, which were carefully checked for (Sikström et al. 2002). They correspond to at least a 95% confidence interval of the various measurements. Due to recombination in the plasma LIF curves for all investigated states were more or less affected by background light. The problem could not be avoided since the metastable platform levels were only populated during the early stage of the plasma evolution. The background was subtracted in the fitting procedure but remains as a major contribution to the error bars in the present measurements.

3. Transition probability and oscillator strength calculations

As the Rh^+ ion belongs to the ruthenium isoelectronic sequence, we considered a relativistic Hartree-Fock model with core-polarization (HFR+CPOL) similar to the one used with success in Ru I (Fivet et al. 2009). More precisely, the configurations included in the configuration interaction expansions were the following: $4d^8 + 4d^75s + 4d^76s + 4d^75d + 4d^76d + 4d^65s^2 + 4d^65p^2 + 4d^65d^2 + 4d^65s6s + 4d^65s5d + 4d^65s6d$ (even parity) and $4d^75p + 4d^76p + 4d^74f + 4d^75f + 4d^65s5p + 4d^65s6p + 4d^65p5d + 4d^65p6s$ (odd parity). The ionic core considered for the core-polarization model potential and the correction to the dipole operator was a Mo-like core, i.e. a $4d^6$ Rh IV core. The dipole polarizability, α_d, for such a core is, according to Fraga et al. (1976), equal to 4.79 a_0^3. For the cut-off radius, r_c, we used the HFR mean value $\langle r \rangle$ of the outermost 4d core orbital, i.e. 1.52 a_0.

Some radial integrals, considered as free parameters, were then adjusted with a least-squares optimization program minimizing the discrepancies between the calculated Hamiltonian eigenvalues and the experimental energy levels from Sancho (1958). More precisely, for the $4d^8$, $4d^75s$ and $4d^75p$ configurations, the average energies (E_{av}), the electrostatic direct (F^k) and exchange (G^k) integrals, the spin-orbit (ζ_{nl}) and the effective interaction (α) parameters were allowed to vary during the fitting process. An additional effective operator (β) for the $4d^75s$ configuration was also included in the adjustment. All other Slater integrals were scaled down by a factor 0.85 following a well-established procedure (Cowan 1981). The designations of the even levels at 8164.4 and 11 643.7 cm^{-1} in Sancho (1958) were interchanged as indicated by the calculations of Shadmi (1961). The even level at 35012.0 cm^{-1} was excluded from the fit because its designation as $4d^7(^2P)5s\ b^3P_0$ by Sancho (1958) appeared questionable. In fact the predicted eigenvalue for this state was found to be more than 1000 cm^{-1} above the experimental value. Actually, the closest even eigenstate with $J = 0$ is $4d^8\ ^1S_0$. Unfortunately, a comparison between the predicted transition probabilities and the intensities observed by Sancho (1958) for the 6 classified lines (of which 2 are doubly classified) involving this level was not conclusive in asserting this alternative designation. The standard deviations of the fits were 50 cm^{-1} for the even parity (35 levels, 12 parameters) and 111 cm^{-1} for the odd parity (84 levels, 9 parameters). The adopted radial parameter values with their standard deviations are given in Table 2.

Theoretical radiative lifetimes obtained in the present study are compared with the experimental values in Table 1. As shown in this table, the agreement between theory and experiment is good. However, the HFR+CPOL lifetimes are systematically about 10% longer than the measurements. This is probably due to the fact that core-polarization effects were slightly overestimated in our physical model. It is worth mentioning that calculated lifetimes were found to decrease by up to 5% when using a dipole polarizability equal to 4.3 a_0^3, i.e. 10% smaller than the one published by Fraga et al. (1976) for Rh IV. It was also verified that a variation of 10% of the cut-off radius did not modify the computed lifetimes.

Considering the experimental lifetime values and the theoretical branching fractions as obtained in the present work, it is possible to derive normalized transition probabilities and oscillator strengths. In Table 3, we present the gA- and $\log gf$-values for the strongest lines ($\log gf > -2.0$) depopulating the levels for which the experimental lifetimes are reported in Table 1.

Table 1. Experimental and calculated lifetimes obtained in the present work for selected levels within the $4d^7(^4F)5p$ configuration of Rh II.

Level	Energy (cm^{-1})[a]	Origin (cm^{-1})[a]	Excitation λ_{vac} (nm)	Conversion[b]	Detection (nm)	τ_{exp}(ns)	τ_{calc}(ns)
z $^5F^\circ_4$	56547.3	18540.4	263.03	3ω +2S	252	3.9 ± 0.5	4.4
z $^5F^\circ_5$	57020.8	18540.4	259.80	3ω +2S	249	3.8 ± 0.3	4.0
z $^5F^\circ_3$	58358.5	19792.4	259.22	3ω +2S	251	3.8 ± 0.3	4.2
z $^5F^\circ_2$	59698.6	20646.9	255.99	3ω +2S	251	3.8 ± 0.3	4.2
z $^5D^\circ_4$	59161.5	16884.8	236.47	3ω +S	246/304	3.3 ± 0.2	3.9
z $^5D^\circ_3$	60448.4	18540.4	238.55	3ω +S	246/303	3.4 ± 0.4	3.9
z $^5D^\circ_2$	61355.9	19792.4	240.52	3ω +S	246/302	3.7 ± 0.5	4.0
z $^5G^\circ_6$	59702.4	16884.8	233.48	3ω +S	233	3.0 ± 0.2	3.1
z $^5G^\circ_5$	59729.4	16884.8	233.33	3ω +S	243	3.5 ± 0.2	4.0
z $^5G^\circ_4$	61173.1	16884.8	225.72	3ω +S	242	3.3 ± 0.2	3.5
z $^5G^\circ_3$	61939.8	18540.4	230.35	3ω +S	242	3.3 ± 0.3	3.6
z $^5G^\circ_2$	62288.3	20646.9	240.07	3ω +S	243/235	3.3 ± 0.3	3.6
z $^3G^\circ_5$	62194.4	16884.8	220.64	3ω	272	3.2 ± 0.2	3.5
z $^3G^\circ_4$	63959.5	18540.4	220.10	3ω	274	3.4 ± 0.2	3.7
z $^3G^\circ_3$	65321.2	18540.4	213.69	3ω	274	2.0 ± 0.2	2.4
z $^3F^\circ_4$	62326.1	16884.8	219.99	3ω	271	2.4 ± 0.2	2.8
z $^3F^\circ_3$	63454.9	18540.4	222.58	3ω	278	2.3 ± 0.3	2.5

Notes. [a] From Sancho (1958); [b] 3ω: frequency tripling, S: Stokes Raman shifting.

Table 2. Adopted radial parameters for the $4d^8$, $4d^75s$ and $4d^75p$ configurations.

Configuration	Parameter	Ab initio (cm^{-1})	Fitted (cm^{-1})	Ratio
$4d^8$	E_{av}	10 882	10 421 ± 21	
	F^2(4d,4d)	65 044	51 938 ± 222	0.80
	F^4(4d,4d)	42 149	35 804 ± 554	0.85
	α	0	21 ± 5	
	ζ_{4d}	1163	1180 ± 20	1.01
$4d^75s$	E_{av}	36 719	37 656 ± 26	
	F^2(4d,4d)	68 421	54 908 ± 332	0.80
	F^4(4d,4d)	44 587	39 300 ± 466	0.88
	α	0	32 ± 2	
	β	0	−462 ± 142	
	ζ_{4d}	1256	1260 ± 10	1.00
	G^2(4d,5s)	13 647	11 376 ± 42	0.83
$4d^75p$	E_{av}	74 500	77 980 ± 16	
	F^2(4d,4d)	69 029	55 106 ± 135	0.80
	F^4(4d,4d)	45 033	38 083 ± 194	0.85
	α	0	24 ± 2	
	ζ_{4d}	1269	1269 ± 15	1.00
	ζ_{5p}	1135	1406 ± 33	1.24
	F^2(4d,5p)	17 482	14 722 ± 134	0.84
	G^1(4d,5p)	7027	5339 ± 57	0.76
	G^3(4d,5p)	5685	3798 ± 144	0.67

4. Conclusions

A new set of transition probabilities and oscillator strengths has been obtained for transitions depopulating 17 levels of Rh II belonging to the $4d^7(^4F)5p$ configuration. These results have been obtained from a combination of experimental lifetimes measured by laser-induced fluorescence spectroscopy and HFR+CPOL branching fractions.

Acknowledgements. This work was financially supported by the Integrated Initiative of Infrastructure Project LASERLAB-EUROPE, contract RII3-CT-2003-506350, the Swedish Research Council through the Linnaeus grant and grant 2006-3085, the Knut and Alice Wallenberg Foundation and the Belgian FRS-FNRS. E.B., P.Q. and P.P. are, respectively, Research Director, Senior Research Associate and Research Associate of the FRS-FNRS. They are grateful to the Swedish team for the warm hospitality enjoyed at the Lund Laser Centre during the measurements.

References

Bergström, H., Faris, H., Hallstadius, G. W., et al. 1988, Z. Phys. D, 8, 17
Biémont, E., Palmeri, P., Quinet, P., et al. 2001, MNRAS, 328, 1085
Corliss, C. H., & Bozman, W. R. 1962, in Nat. Bur. Stand. Monogr. (Washington DC: US Department of Commerce), 53
Cowan, R. D. 1981, The Theory of Atomic Structure and Spectra (Berkeley: California University Press)
Cowley, C. R. 2009, http://www.astro.lsa.umich.edu~/cowley
Fivet, V., Quinet, P., Palmeri, P., et al. 2009, MNRAS, 396, 2124
Fraga, S., Karwowski, J., & Saxena, K. M. S. 1976, Handbook of Atomic Data (Amsterdam: Elsevier)
Lundberg, H., Johansson, S., Litzén, U., Wahlgren, G. M., & Leckrone, S. 1998, in The Scientific Impact of the Goddard High Resolution Spectrograph, ASP Conf. Ser., 143, 343
Meggers, W. F., Corliss, C. H., & Scribner, B. F. 1975, Nat. Bur. Stand. NBS, Monograph (Washington DC: US Department of Commerce), 145
Moore, C. E. 1971, Nat. Stand. Ref. Data Ser. NSRDS-NBS, 35, III
Moore, C. E., Minnaert, M. G. J., & Houtgast, J. 1966, The Solar Spectrum 2935 Å to 8770 Å, NBS Monograph 61 (Washington DC: US Department of Commerce)
Nilsson, H., Hartman, H., Engström, L., et al. 2010, A&A, 511, A16
Quinet, P., Palmeri, P., Biémont, E., et al. 1999, MNRAS, 307, 934
Quinet, P., Biémont, E., Palmeri, P., et al. 2011, J. Elec. Spectr. Rel. Phen., 184, 174
Reader, J., Corliss, C. H., Wiese, W. L., & Martin, G. A. 1980, Nat. Stand. Ref. Data Ser. NSRDS-NBS, 68
Sancho, F. J. 1958, Anales Real. Soc. Esp. Fis. Quim., 54A, 41
Shadmi, Y. 1961, Bull. Res. Council Israel, 9F, 141
Sikström, C. M., Nilsson, H., Litzén, U., Blom, A., & Lundberg, H. 2002, J. Quant. Spec. Radiat. Transf., 74, 355
Xu, H. L., Persson, A., Svanberg, S., et al. 2004, Phys. Rev. A, 70, 042508
Zhang, Z. G., Li, Z. S., Svanberg, S., et al. 2001, Eur. Phys. J. D, 15, 301

Table 3. Transition probabilities and oscillator strengths for Rh II selected lines. $X(Y)$ stands for $X \times 10^{Y}$. Only transitions with $\log gf \geq -2.0$ are listed in the table.

λ^a (nm)	Int.[a]	Lower level[a]		Upper level[a]		HFR+CPOL[b]		Normalized[c]	
		E (cm^{-1})	Desig.	E (cm^{-1})	Desig.	gA (s^{-1})	$\log gf$	gA (s^{-1})	$\log gf$
153.091	100	0.0	a^3F_4	65321.2	$z^3G^\circ_3$	8.55(8)	–0.52	1.03(9)	–0.44
156.348	100	0.0	a^3F_4	63959.5	$z^3G^\circ_4$	1.71(8)	–1.20	1.86(8)	–1.17
157.591	100	0.0	a^3F_4	63454.9	$z^3F^\circ_3$	2.17(8)	–1.09	2.36(8)	–1.06
158.932	90	2401.3	a^3F_3	65321.2	$z^3G^\circ_3$	1.92(8)	–1.14	2.30(8)	–1.06
160.445	500	0.0	a^3F_4	62326.1	$z^3F^\circ_4$	1.14(9)	–0.36	1.33(9)	–0.29
160.786	100	0.0	a^3F_4	62194.4	$z^3G^\circ_5$	1.02(8)	–1.40	1.12(8)	–1.36
162.447	200	2401.3	a^3F_3	63959.5	$z^3G^\circ_4$	6.06(7)	–1.62	6.59(7)	–1.58
163.472	200	0.0	a^3F_4	61173.1	$z^5G^\circ_4$	2.76(8)	–0.96	2.93(8)	–0.93
163.788	200	2401.3	a^3F_3	63454.9	$z^3F^\circ_3$	6.72(8)	–0.57	7.30(8)	–0.53
166.876	100	2401.3	a^3F_3	62326.1	$z^3F^\circ_4$	1.66(8)	–1.16	1.94(8)	–1.09
167.019	90	3580.7	a^3F_2	63454.9	$z^3F^\circ_3$	1.39(8)	–1.24	1.51(8)	–1.20
167.422	100	0.0	a^3F_4	59729.4	$z^5G^\circ_5$	1.41(8)	–1.23	1.61(8)	–1.17
167.958	50	2401.3	a^3F_3	61939.8	$z^5G^\circ_3$	1.11(8)	–1.33	1.21(8)	–1.29
170.337	50	3580.7	a^3F_2	62288.3	$z^5G^\circ_2$	4.60(7)	–1.70	5.02(7)	–1.66
174.958	100	8164.4	a^1D_2	65321.2	$z^3G^\circ_3$	1.74(8)	–1.10	2.09(8)	–1.02
176.842	100	0.0	a^3F_4	56547.3	$z^5F^\circ_4$	2.47(7)	–1.93	2.79(7)	–1.88
180.864	100	8164.4	a^1D_2	63454.9	$z^3F^\circ_3$	1.63(8)	–1.10	1.77(8)	–1.06
186.298*		11643.7	a^3P_2	65321.2	$z^3G^\circ_3$	8.76(7)	–1.34	1.05(8)	–1.26
193.008*		11643.7	a^3P_2	63454.9	$z^3F^\circ_3$	4.45(7)	–1.60	4.84(7)	–1.57
213.696*		18540.4	a^5F_4	65321.2	$z^3G^\circ_3$	1.33(7)	–2.04	1.60(7)	–1.96
219.996	200	16884.8	a^5F_5	62326.1	$z^3F^\circ_4$	9.18(7)	–1.17	1.07(8)	–1.11
220.102	100	18540.4	a^5F_4	63959.5	$z^3G^\circ_4$	7.78(7)	–1.25	8.47(7)	–1.21
220.635	100	16884.8	a^5F_5	62194.4	$z^3G^\circ_5$	9.13(7)	–1.18	9.99(7)	–1.14
223.771	50	20646.9	a^5F_2	65321.2	$z^3G^\circ_3$	2.85(8)	-0.67	3.42(8)	–0.59
225.724	80	16884.8	a^5F_5	61173.1	$z^5G^\circ_4$	3.35(7)	–1.59	3.55(7)	–1.57
226.343	50	19792.4	a^5F_3	63959.5	$z^3G^\circ_4$	7.51(8)	-0.24	8.17(8)	-0.20
228.316	20	18540.4	a^5F_4	62326.1	$z^3F^\circ_4$	1.91(7)	–1.82	2.23(7)	–1.76
228.957	20	19792.4	a^5F_3	63454.9	$z^3F^\circ_3$	3.88(7)	–1.52	4.22(7)	–1.48
229.004	300	18540.4	a^5F_4	62194.4	$z^3G^\circ_5$	1.85(9)	0.16	2.02(9)	0.20
230.347	20	18540.4	a^5F_4	61939.8	$z^5G^\circ_3$	2.17(7)	–1.76	2.37(7)	–1.73
233.330	300	16884.8	a^5F_5	59729.4	$z^5G^\circ_5$	1.79(8)	–0.83	2.05(8)	–0.78
233.477	1000	16884.8	a^5F_5	59702.4	$z^5G^\circ_6$	4.18(9)	0.53	4.32(9)	0.55
233.530	10	20646.9	a^5F_2	63454.9	$z^3F^\circ_3$	1.14(8)	–1.03	1.24(8)	–0.99
234.489	80	18540.4	a^5F_4	61173.1	$z^5G^\circ_4$	1.34(7)	–1.96	1.42(7)	–1.93
235.035	100	19792.4	a^5F_3	62326.1	$z^3F^\circ_4$	1.44(8)	–0.92	1.68(8)	–0.86
236.467	100	16884.8	a^5F_5	59161.5	$z^5D^\circ_4$	1.17(8)	–1.00	1.38(8)	-0.94
238.545	200	18540.4	a^5F_4	60448.4	$z^5D^\circ_3$	8.21(7)	–1.15	9.42(7)	–1.10
240.071	80	20646.9	a^5F_2	62288.3	$z^5G^\circ_2$	4.73(7)	–1.39	5.16(7)	–1.35
240.522	150	19792.4	a^5F_3	61355.9	$z^5D^\circ_2$	1.09(8)	–1.02	1.18(8)	–0.99
241.584	500	19792.4	a^5F_3	61173.1	$z^5G^\circ_4$	1.80(9)	0.20	1.91(9)	0.22
242.100	500	20646.9	a^5F_2	61939.8	$z^5G^\circ_3$	1.62(9)	0.15	1.77(9)	0.19
242.709	300	18540.4	a^5F_4	59729.4	$z^5G^\circ_5$	1.54(9)	0.14	1.76(9)	0.19
243.185	300	21180.0	a^5F_1	62288.3	$z^5G^\circ_2$	1.20(9)	0.02	1.31(9)	0.06
245.571	200	20646.9	a^5F_2	61355.9	$z^5D^\circ_2$	1.00(9)	–0.04	1.08(9)	–0.01
245.890	300	19792.4	a^5F_3	60448.4	$z^5D^\circ_3$	1.57(9)	0.16	1.80(9)	0.21
246.103	300	18540.4	a^5F_4	59161.5	$z^5D^\circ_4$	2.09(9)	0.28	2.47(9)	0.35
248.829	50	21180.0	a^5F_1	61355.9	$z^5D^\circ_2$	1.84(7)	–1.77	1.99(7)	–1.73
249.079	150	16884.8	a^5F_5	57020.8	$z^5F^\circ_5$	2.60(9)	0.39	2.67(9)	0.39
250.276	50	25376.9	b^3F_4	65321.2	$z^3G^\circ_3$	2.53(8)	–0.62	3.04(8)	–0.55
250.512	100	19792.4	a^5F_3	59698.6	$z^5F^\circ_2$	9.82(8)	–0.03	1.09(9)	0.01
251.065	100	18540.4	a^5F_4	58358.5	$z^5F^\circ_3$	1.43(9)	0.13	1.58(9)	0.17
252.052	100	16884.8	a^5F_5	56547.3	$z^5F^\circ_4$	1.79(9)	0.24	2.02(9)	0.28
255.992	100	20646.9	a^5F_2	59698.6	$z^5F^\circ_2$	1.44(8)	–0.85	1.59(8)	–0.81
259.216	100	19792.4	a^5F_3	58358.5	$z^5F^\circ_3$	1.24(8)	–0.90	1.37(8)	–0.86
259.540	60	21180.0	a^5F_1	59698.6	$z^5F^\circ_2$	2.33(7)	–1.63	2.58(7)	–1.58
259.795	10	18540.4	a^5F_4	57020.8	$z^5F^\circ_5$	1.04(7)	–1.98	1.07(7)	–1.97
262.541	150	25376.9	b^3F_4	63454.9	$z^3F^\circ_3$	9.81(8)	0.01	1.07(9)	0.04
263.033	100	18540.4	a^5F_4	56547.3	$z^5F^\circ_4$	1.38(8)	–0.84	1.56(8)	–0.79
263.900*		27439.4	b^3F_3	65321.2	$z^3G^\circ_3$	2.26(8)	-0.63	2.71(8)	-0.55
265.093	30	20646.9	a^5F_2	58358.5	$z^5F^\circ_3$	1.50(7)	–1.80	1.66(7)	–1.76
266.448	50	27801.4	a^5P_3	65321.2	$z^3G^\circ_3$	6.44(7)	–1.16	7.73(7)	–1.08
270.560	150	25376.9	b^3F_4	62326.1	$z^3F^\circ_4$	1.53(9)	0.23	1.79(9)	0.29

Table 3. continued.

λ^a (nm)	Int.^{a}	Lower level^a		Upper level^a		HFR+CPOL^b		Normalized^c	
		E (cm^{-1})	Desig.	E (cm^{-1})	Desig.	gA (s^{-1})	log gf	gA (s^{-1})	log gf
271.527	150	25376.9	b^3F_4	62194.4	$z^3G^\circ_5$	1.11(9)	0.09	1.21(9)	0.13
273.420	10	25376.9	b^3F_4	61939.8	$z^5G^\circ_3$	1.41(7)	–1.80	1.54(7)	–1.76
273.740	150	27439.4	b^3F_3	63959.5	$z^3G^\circ_4$	1.11(9)	0.10	1.21(9)	0.13
273.992	150	28834.6	b^3F_2	65321.2	$z^3G^\circ_3$	6.61(8)	–0.13	7.93(8)	–0.05
276.483	100	27801.4	a^5P_3	63959.5	$z^3G^\circ_4$	2.09(8)	–0.62	2.27(8)	–0.58
277.577	100	27439.4	b^3F_3	63454.9	$z^3F^\circ_3$	2.67(8)	–0.51	2.90(8)	–0.47
279.278	100	25376.9	b^3F_4	61173.1	$z^5G^\circ_4$	9.25(7)	-0.97	9.81(7)	–0.94
280.395	80	27801.4	a^5P_3	63454.9	$z^3F^\circ_3$	5.93(7)	–1.16	6.45(7)	–1.12
285.049	50	25376.9	b^3F_4	60448.4	$z^5D^\circ_3$	2.00(7)	–1.61	2.29(7)	–1.55
286.560	30	27439.4	b^3F_3	62326.1	$z^3F^\circ_4$	2.45(7)	–1.52	2.86(7)	–1.45
289.560	2	27801.4	a^5P_3	62326.1	$z^3F^\circ_4$	1.38(7)	–1.76	1.61(7)	–1.69
289.763	100	27439.4	b^3F_3	61939.8	$z^5G^\circ_3$	3.61(7)	–1.34	3.94(7)	–1.30
291.015	200	25376.9	b^3F_4	59729.4	$z^5G^\circ_5$	8.48(8)	0.03	9.69(8)	0.09
292.680	100	28131.4	a^5P_2	62288.3	$z^5G^\circ_2$	1.10(7)	–1.85	1.20(7)	–1.81
292.838	40	27801.4	a^5P_3	61939.8	$z^5G^\circ_3$	2.67(7)	–1.47	2.91(7)	–1.43
294.756	30	27439.4	b^3F_3	61355.9	$z^5D^\circ_2$	2.04(7)	–1.57	2.21(7)	–1.54
296.354	200	27439.4	b^3F_3	61173.1	$z^5G^\circ_4$	2.92(8)	–0.41	3.10(8)	–0.39
298.830	40	28834.6	b^3F_2	62288.3	$z^5G^\circ_2$	6.77(7)	–1.05	7.39(7)	–1.00
299.563	15	27801.4	a^5P_3	61173.1	$z^5G^\circ_4$	1.90(7)	–1.59	2.02(7)	–1.57
300.898	80	28131.4	a^5P_2	61355.9	$z^5D^\circ_2$	6.09(7)	–1.08	6.58(7)	–1.05
301.978	100	28834.6	b^3F_2	61939.8	$z^5G^\circ_3$	1.10(8)	–0.82	1.20(8)	–0.79
302.857	80	27439.4	b^3F_3	60448.4	$z^5D^\circ_3$	1.16(7)	–1.79	1.33(7)	–1.74
305.565	80	32604.7	a^3G_4	65321.2	$z^3G^\circ_3$	4.56(7)	–1.20	5.47(7)	–1.12
306.223	60	27801.4	a^5P_3	60448.4	$z^5D^\circ_3$	1.99(7)	–1.55	2.28(7)	–1.49
309.344	100	28131.4	a^5P_2	60448.4	$z^5D^\circ_3$	4.96(7)	–1.15	5.69(7)	–1.09
309.675	80	29073.0	a^5P_1	61355.9	$z^5D^\circ_2$	2.64(7)	–1.42	2.85(7)	–1.39
310.191	15	31730.5	a^3G_5	63959.5	$z^3G^\circ_4$	1.73(7)	–1.60	1.88(7)	–1.57
313.417	10	27801.4	a^5P_3	59698.6	$z^5F^\circ_2$	6.43(6)	–2.02	7.11(6)	–1.98
315.144	40	27439.4	b^3F_3	59161.5	$z^5D^\circ_4$	9.82(6)	–1.83	1.16(7)	–1.76
315.926	200	25376.9	b^3F_4	57020.8	$z^5F^\circ_5$	1.06(8)	–0.80	1.09(8)	–0.79
316.230	20	28834.6	b^3F_2	60448.4	$z^5D^\circ_3$	8.83(6)	–1.88	1.01(7)	–1.82
316.691	100	28131.4	a^5P_2	59698.6	$z^5F^\circ_2$	1.89(7)	–1.55	2.09(7)	–1.50
318.783	150	27801.4	a^5P_3	59161.5	$z^5D^\circ_4$	7.48(7)	–0.94	8.84(7)	–0.87
320.725	100	25376.9	b^3F_4	56547.3	$z^5F^\circ_4$	4.56(7)	–1.15	5.14(7)	–1.10
323.332	100	27439.4	b^3F_3	58358.5	$z^5F^\circ_3$	3.24(7)	–1.29	3.58(7)	–1.25
323.895	20	28834.6	b^3F_2	59698.6	$z^5F^\circ_2$	8.25(6)	–1.89	9.12(6)	–1.84
324.049	5	32604.7	a^3G_4	63454.9	$z^3F^\circ_3$	2.19(7)	–1.47	2.38(7)	–1.43
326.427	20	29073.0	a^5P_1	59698.6	$z^5F^\circ_2$	7.02(6)	–1.95	7.76(6)	–1.91
326.756	150	31730.5	a^3G_5	62326.1	$z^3F^\circ_4$	7.07(7)	–0.94	8.25(7)	–0.88
330.734*		28131.4	a^5P_2	58358.5	$z^5F^\circ_3$	2.74(7)	–1.35	3.03(7)	–1.30
336.361*		32604.7	a^3G_4	62326.1	$z^3F^\circ_4$	5.34(6)	–2.04	6.23(6)	–1.98
339.547*		31730.5	a^3G_5	61173.1	$z^5G^\circ_4$	1.46(7)	–1.60	1.55(7)	–1.57
340.791*		32604.7	a^3G_4	61939.8	$z^5G^\circ_3$	7.00(6)	–1.92	7.64(6)	–1.88
343.451*		27439.4	b^3F_3	56547.3	$z^5F^\circ_4$	1.09(7)	–1.71	1.23(7)	–1.66
345.266*		36366.3	c^3P_2	65321.2	$z^3G^\circ_3$	1.19(7)	–1.67	1.43(7)	–1.59
347.776*		27801.4	a^5P_3	56547.3	$z^5F^\circ_4$	3.86(7)	–1.15	4.35(7)	–1.10
352.232*		36938.9	a^3D_3	65321.2	$z^3G^\circ_3$	1.01(7)	–1.73	1.21(7)	–1.65
369.054*		36366.3	c^3P_2	63454.9	$z^3F^\circ_3$	5.34(6)	–1.96	5.80(6)	–1.93
377.024*		36938.9	a^3D_3	63454.9	$z^3G^\circ_3$	9.37(6)	–1.70	1.02(7)	–1.66
391.561*		36794.5	a^3H_5	62326.1	$z^3F^\circ_4$	5.05(6)	–1.93	5.89(6)	–1.87
417.555*		35787.2	a^3H_6	59729.4	$z^5G^\circ_5$	3.49(6)	–2.04	3.99(6)	–1.98

Notes. [(a)] From Sancho (1958). Wavelengths are given in vacuum and in air below and above 200 nm, respectively. Starred values are deduced from experimental levels. [(b)] This work : HFR+CPOL calculations (see the text). [(c)] This work : HFR+CPOL values normalized by the laser measurements of the present work (see the text).